Nanoscale

PAPER

Quantum dots cause acute systemic toxicity in lactating rats and growth restriction of offspring†

Cite this: DOI: 10.1039/c8nr01248b

Lin Yang,[a,b] Huijuan Kuang,[a] Wanyi Zhang,[a,c] Wei Hua[a] and Hengyi Xu *[a]

Received 10th February 2018,
Accepted 23rd May 2018

DOI: 10.1039/c8nr01248b

rsc.li/nanoscale

The *in vivo* toxicity of QDs in animals has been broadly studied; however, their reproductive toxicity towards lactating rodents is currently unknown. This study therefore aims to assess the potential toxicity against dams and offspring after postnatal QD exposure at two doses (5 and 1 nmol per rat) and unravel whether QDs can translocate to pups *via* breastfeeding. The dose-dependent systemic toxicity of QDs in dams was observed by examining the body weight, hematology, biochemistry, histopathological changes, and sex hormone levels. It was found that the QDs primarily accumulated in the liver and spleen of dams at 1 day post injection (dpi), but the highest concentrations were found in the kidneys at 18 dpi. A few QDs were detected in breast milk and stomach and intestine of pups; this suggested that the QDs were transmitted to breast milk *via* blood circulation and then transferred to pups *via* breastfeeding. High-dose QDs induced severe growth inhibition and a 71.08% offspring mortality, while pups showed growth restriction within 90 dpi in the low-dose group. Moreover, the hematology, biochemistry, and histology results showed limited chronic toxicity against offspring in the long term. This study provides a theoretical foundation for the exposure assessment of nanomaterials in lactating animals and for the advancement of QDs in the biomedical field.

Background

Quantum dots (QDs) are extraordinary semiconductor nanocrystals with unique optical and electronic properties, such as size-tunable fluorescence, narrow emission and wide absorption spectra, high luminescence quantum yields, and remarkable photostability, and have been considered as alternatives to traditional organic dyes in many biology and biomedicine applications.[1,2] QDs are also beneficial in biosensing, cellular and molecular labeling and tracking, deep-tissue imaging, cancer targeting, and disease diagnosis and therapy.[3–9] However, QDs at the nanoscale size possess high particle reactivity due to their relatively large surface area to volume ratio when compared with their micrometric counterpart; this causes intense QD biological interactions in cells or animals.[10] Furthermore, most QDs, including cadmium selenide (CdSe) or cadmium telluride (CdTe) nanoparticles (NPs), used in nanomedicines contain cadmium, which is carcinogen and has deleterious effects on the reproductive tissues and embryos.[11,12] Any potential pharmacological and toxicological effects of QDs should be therefore comprehensively explored before reaching the clinic. Despite the increasing understanding of QD toxicity in both cell cultures and animal models, knowledge is still scarce, particularly in the reproductive and developmental system, and is even sometimes contradictory.

Cell cultures for probing the toxic effects and mechanisms of QDs *in vitro* have been widely explored.[13–16] QDs cause cellular damage *via* the release of toxic metal ions and generation of reactive oxygen species (ROS). Moreover, QDs at very high concentrations (40 pM, 25 mg kg^{-1}) have shown no appreciable toxicity in *in vivo* animal models including mice,[17,18] rats,[19] and rhesus macaques.[20] However, QDs are stored in the mononuclear phagocyte system (MPS), including the liver, spleen, and lymphatic system, and are deposited in living animals for up to two years.[18,21] The size-dependent elimination rate of QDs was also observed in rats,[22] whereby QDs less than 5.5 nm could be rapidly and efficiently eliminated from the body through urinary excretion, whereas QDs sized over 15 nm prevented renal excretion. Of note, developing embryos and young offspring are highly sensitive to environmental hazards and NPs that may have insignificant effects on adult individuals. The health effect of NPs on both the maternal reproductive system and the next generation has aroused much concern because NPs, such as QDs, silver NPs, and tita-

[a]State Key Laboratory of Food Science and Technology, Nanchang University, Nanchang 330047, China. E-mail: kidyxu@163.com, HengyiXu@ncu.edu.cn; Fax: +86-791-8830-4400; Tel: +86-791-8830-4447-ext-9520
[b]Comprehensive Pneumology Center (CPC), Institute of Lung Biology and Disease, Helmholtz Zentrum München, Munich, Ingolstaedter Landstrasse 1, 85764 Neuherberg/Munich, Germany
[c]The Second Affiliated Hospital of Nanchang University, Nanchang 330000, China
†Electronic supplementary information (ESI) available. See DOI: 10.1039/c8nr01248b

nium dioxide NPs, can be stored in the body long term and may bestow high reactivity and unique translocational properties.[23–46]

Currently, scientific efforts are concentrated on determining the effects of NPs on the female reproductive system and embryo development *in vivo*.[28,32,34,35,39,43–46] Yamashita *et al.* found that silica NPs could penetrate into the rodent placenta and transferred to the fetuses, resulting in structural and functional damages in the placenta as well as the inhibition of fetal growth.[23] Chu *et al.* reported that prenatal exposure to CdTe/CdS QDs could migrate from pregnant mice to their fetuses across the placental barrier,[26] whereas we found that amphiphilic polymer-coated CdSe/ZnS QDs (20 nm) were effectively blocked by the placental barrier in our recent study.[46] Moreover, sliver NPs,[32] gold NPs,[28,41] titanium dioxide NPs,[35,40] and carbon nanotubes[29,39,43] have been shown to cross the placental barrier and cause various degrees of fetal toxicity. For instance, the size-dependent translocation of gold NPs from the maternal blood into the fetus was observed, suggesting that gold NPS sized less than 20–25 nm mainly cross the placenta *via* transtrophoblastic channels.[28] Unfortunately, most studies to date focused on pregnant animal models ignore the side effects of NP exposure during the lactation period. Recently, silver NPs were found in breast milk and in the brains of pups and it was also found that titanium dioxide NPs damaged the tight junction of the blood–milk barrier.[44,45,47] However, these studies lacked biodistribution profiles of NPs in dams, gastrointestinal examination of NPs in pups, and a systemic growth and development analysis of offspring in the long term.

The aim of the present study was therefore to assess whether QDs were able to translocate to offspring *via* breastfeeding or not and to elucidate further the tissue distribution and toxicity profiles of QDs in dams and the long-term effects on offspring, following a two-time intravenous injection postnatal day 2 (PD2) and day 3 (PD3). The case of intravenous exposure showed a high amount of QDs distributed throughout the body compared to with oral or inhalation administration, leading to an easier detection of cadmium contents in the breast milk of dams or in the gastrointestinal tract and liver of pups. QDs belong to typical NPs with enormous potential applications in clinical settings and have shown insufficient toxicity in nonhuman primates (rhesus macaques) and small animals (mice and rats). Most studies also reported that NPs, including QDs, could cross the placental barrier as well as impair the structures and functions of the placenta and embryo development. Accordingly, we utilized two dosages of 20 nm QDs, coated with reactive carboxyl group, to assess the toxicological effects in dams and offspring during postnatal exposure. More specifically, inductively coupled plasma mass spectrometry (ICP-MS) was used to examine the cadmium contents in widespread organs, milk, blood, and feces of dams, and the stomach, intestine, liver, kidney, and spleen of offspring. Blood biochemistry and hematology and pathological examinations were performed to determine the inflammatory response, potential tissue damage, inflammation, or lesion in dams. Furthermore, the maternal endocrine function was determined by inspecting the concentrations of sex hormones, including estradiol (E_2), progesterone (P_4), luteinizing hormone (LH), follicle stimulating hormone (FSH), and prolactin (PRL). Meanwhile, offspring growth and development were evaluated from birth up to 180 days after exposure by measuring the survival rate, body weight (BW), and organ index, and conventional toxicological analysis was also conducted.

Methods

Materials

The amphiphilic polymers with surface reactive carboxyl group-coated CdSe/ZnS QDs used here provided by Ocean NanoTech, LLC (San Diego, CA). The size of QDs was analyzed by transmission electron microscopy (TEM) prior to use. Briefly, the NP samples were prepared by dropping a sample onto an agar carbon-coated copper grid (400 mesh) and then the solvent was evaporated. The images were obtained at 50–100 K magnifications with a JEOL TEM (JEOL USA, Inc. Peabody, MA) operating at 100 kV as previously described.[48,49] The hydrodynamic diameter distributions of the QDs (n = 6) and zeta potential were measured by dynamic light scattering (DLS) using a Zetatrac Ultra 151 (Microtrac Inc., Montgomeryville, PA).

Animal studies

Healthy adult female and male Sprague–Dawley (SD) rats (10–12 weeks old) were purchased from the Experimental Animal Center of Nanchang University, China. The animals were raised in an animal facility at 25 °C with a 12 h light/dark cycle; the animals were supplemented with food and water *ad libitum*. All the procedures involving the animals were approved by the Animal Care Review Committee (approval number 0064257), Nanchang University, Jiangxi, China, and were carried out in line with the Institutional Animal Care Committee guidelines. Twenty-eight female rats with body masses between 300 g and 350 g were mated with 14 male rats housed in fourteen stainless steel cages (one cage housed one male rat and two female rats). Pregnant rats were confirmed by the presence of vaginal plugs and daily BW examination, and then the female rats were randomly divided into three groups: 9 rats in the high-dose group treated with 5 nmol QDs per rat (14.28–16.67 nmol kg^{-1}), 10 rats in the low-dose group treated with 1 nmol QDs per rat (2.85–3.33 nmol kg^{-1}), and 9 rats in the vehicle control group treated with physiological saline. Exposures were performed in PD2 and PD3 *via* two tail-vein injections of 5 μM or 1 μM QDs or saline in a total volume of 1 mL. The QDs dosage used here was according to the biological response and close to the doses applied in early studies.[19,50,51] Also, the accumulated dose of QDs in various organs was parallel to those assessed in previous *in vivo* QD imaging and toxicological studies, as enumerated in Table S1.†

Acute and subacute toxicity evaluation on maternal rats

To assess the acute and subacute systemic toxicities of QDs in dams, the rats' BWs, food consumption, and survival rates were recorded throughout the entire experimental period. The rates of BW change were calculated using eqn (1):

$$\text{Rates of BW change} = \frac{\text{Present BW} - \text{BW of the start day (g)}}{\text{BW of the start day (g)}} \times 100\%. \quad (1)$$

Three and six rats from each group were sacrificed at 1 and 18 day post injection (dpi), respectively, and various organ samples were collected and weighed for visceral index measurement. The organ index was calculated using eqn (2):

$$\text{Organ index} = \frac{\text{Mass of organs (mg)}}{\text{Mass of body weight (g)}}. \quad (2)$$

Samples of the organs were isolated and a small portion of tissue was immediately fixed in 10% neutral buffered formalin for histological examination. Portions from each organ (0.2–0.5 g) were stored at −20 °C for cadmium elemental analysis. Also, blood and feces samples were collected from the three lactating rats of each group at 1, 5, 10, and 18 dpi. Breast milk was harvest from the other 4 or 3 rats' nipples of each group at 2, 9, and 16 dpi, except for the high-dose group as 3 rats had died after injection.

Blood biochemistry and hematology: blood samples were harvest from each group at four time points after injection. Briefly, the blood samples were collected from the orbital venous plexus using a capillary glass tube that pierced the inner canthus without affecting the rats living, and approximately 0.3 mL whole blood was collected in potassium EDTA collection tube for hematology assay, and 0.7 mL blood was centrifuged to obtain over 0.25 mL serum for the biochemistry assay. The whole blood samples that were treated with the anticoagulant and the blood serum were examined at the First Affiliated Hospital of Nanchang University, Nanchang, China. When the rats were sacrificed at 1 and 18 dpi, the whole blood samples, apart from the part used for the biochemistry and hematology analysis, were collected for determination of the cadmium content and the serum sex hormones level.

Histopathological examinations. The dams were sacrificed utilizing 10% chloral hydrate anesthetic, followed by exsanguination at 1 and 18 dpi, and a small portion of each organ (liver, spleen, kidney, lung, brain, heart, intestine, and uterus) was fixed in 10% neutral buffered formalin according to our previous study.[49] Subsequently, the isolated tissues were embedded in paraffin blocks (previously melted at 58 °C) and frozen at 4 °C before 3–5 μm sections were cut and stained with hematoxylin and eosin (H&E) for pathological examination. An Olympus optical microscope (Tokyo, Japan) was used to observe the stained slices.

Sex hormone assays. Various sex hormones, including E_2, P_4, LH, FSH, and PRL, in the serum of lactating rats were collected at 1 and 18 dpi and measured using commercial kits (JiuDing Biomedical engineering Ltd, China). The biochemical assays were performed with a gamma counter RIA program (Type 7170A; Hitachi Co, Japan).

Quantitative measurement of Cd levels in the maternal and offspring tissues

The tissue samples of dams (the liver, kidney, spleen, lung, heart, brain, stomach, intestine, and breast) were carefully collected and frozen. The breast milk was collected from the mammary glands of dams in the low-dose group and control group using a tailor-made pipette following 10% chloral hydrate and oxytocin intraperitoneal injections at 2, 9, 16 dpi. The offsprings' stomach, intestine, liver, kidney, and spleen were harvested at 1, 5, 10, 18, 60, 120, and 180 dpi. The subsamples of approximately 0.2–0.5 g tissue, including feces and blood, were isolated and dissolved in 12 mL digestion solution ($HNO_3 : HClO_4 = 5 : 1$) with heating at 230 °C. The temperature was increased to 280 °C when the reaction reached equilibrium. The digested samples were diluted with Milli-Q water to 25 mL after removal from the heating block, and subsequently were used to determine the cadmium concentrations with ICP-MS. The linearities of the calibration curves of ^{114}Cd with ICP-MS with 1, 2, 5, 10, 20, and 50 ng mL^{-1} of standard solution ($R^2 > 0.999$), and with 0.02, 0.05, 0.1, 0.5, 1, and 2 ng mL^{-1} of standard solution ($R^2 > 0.999$), for determining the cadmium concentrations in dam samples and offspring samples, respectively, were both good. The concentrations of Cd and the percentages of Cd (Y) in different tissues were calculated using eqn (3) and (4), respectively:

$$[\text{cadmium } (\mu g\, g^{-1})] \text{ in tissue} = \frac{[\text{Cd}]\text{in tissue suspenion} \times 25}{\text{wet weight of tissue}} \quad (3)$$

$$Y = \frac{[\text{Cd}] \text{ in tissue suspenion} \times 25 \times \text{organ weight}}{\text{wet weight of tissue} \times \text{total injected cadmium}} \times 100\%. \quad (4)$$

Acute and chronic toxicity analysis in offspring

To evaluate the long-term effects on offspring when dams were exposed to QDs, the pups' BW, body length, tail length, survival rate, morphology inspection were examined during the breastfeeding period. Furthermore, to explore potential side effects in the next generation, blood biochemistry and hematology analysis and histological examination as well as organ index and BW were carried out for up to 180 days after exposure.

Statistical analysis

Data are presented herein as the mean ± standard error ($n \geq 3$). Comparisons of the results among three groups or between two groups were carried out by one-way analysis of variance (ANOVA) and L.S.D. test, or student t tests as two-sided using SPSS v16.0 (SPSS, Inc., Chicago, IL); $p < 0.05$ and $p < 0.01$ were considered statistically significant and highly statistically significant, respectively.

Results and discussion

Characterization of the CdSe/ZnS QDs

The hydrodynamic size distribution of the QDs in water determined by DLS was 20 ± 6.05 nm, which was slightly larger than the corresponding size (13 nm) from TEM measurements (Fig. 1). The used QDs exhibited a uniform, spherical, and monodispersed state under TEM. The different surface states and hydration degrees of the NP samples contributed to a slight deviation in the diameter measured by TEM and DLS according to several previous studies.[10,48–51] The QDs were well-resolved in water and DLS measurements of both the core and coating showed a bigger diameter. The absorption spectrum of the QDs ranged from 400 to 600 nm and the maximum emission peak was at 580 nm.

Acute and subacute systemic toxicity of the QDs in lactating rats

Acute and subacute toxicities were determined following i.v. injection of two QDs doses of 2.5 nmol day^{-1} and 0.5 nmol day^{-1} for two consecutive days. The flow diagram of the experiment is shown in Fig. 1d. Three or six living female rats were planned to be sacrificed at 1 (PD4) and 18 dpi (PD21) as the litters were weaned around day 21 after delivery. Unfortunately, in the high-dose group, one rat died after the first injection, and two others died following the second injection prior to examination. For other groups, no animal deaths occurred throughout the experimental period (Fig. 2d). Physical behavior, the rates of BW change, and food consumption of the dams were then performed for the surviving rats. Fig. 2 displays that rats in the high-dose group showed a BW loss after the first injection (−5.36 ± 1.96%), which continued to decrease until 5 dpi with a maximum loss of −9.30 ± 0.58% at 3 dpi. The low-dose group only lost weight at 1 dpi (−2.51 ± 1.88%) and 3 dpi (−1.39 ± 2.71%), representing a significant difference from the control group. After 5 dpi, no significant difference of the rates of BW change in the three groups were observed, but both QD-treated groups still presented slow increasing trends. By contrast, recent QDs toxicological studies demonstrated that 0.4 nmol, 15 nmol, and 25 mg kg^{-1} QDs did not cause great effects on the BW of mice, rats, and monkeys, respectively,[19,20,52] suggesting lactating animals might be particularly vulnerable to QDs exposure. Analysis of food consumption in Fig. 2b found only 6.83 ± 2.07 g, 5.06 ± 0.16 g, 10.44 ± 5.04 g, and 23.34 ± 3.22 g food was ingested per day from 0 to 3 dpi in the high-dose group, which showed a noticeable lower food intake than the control or the low-dose group with at least 34.07 ± 8.08 g of food intake per day. This indicated the eating behavior of the rats in the high-dose

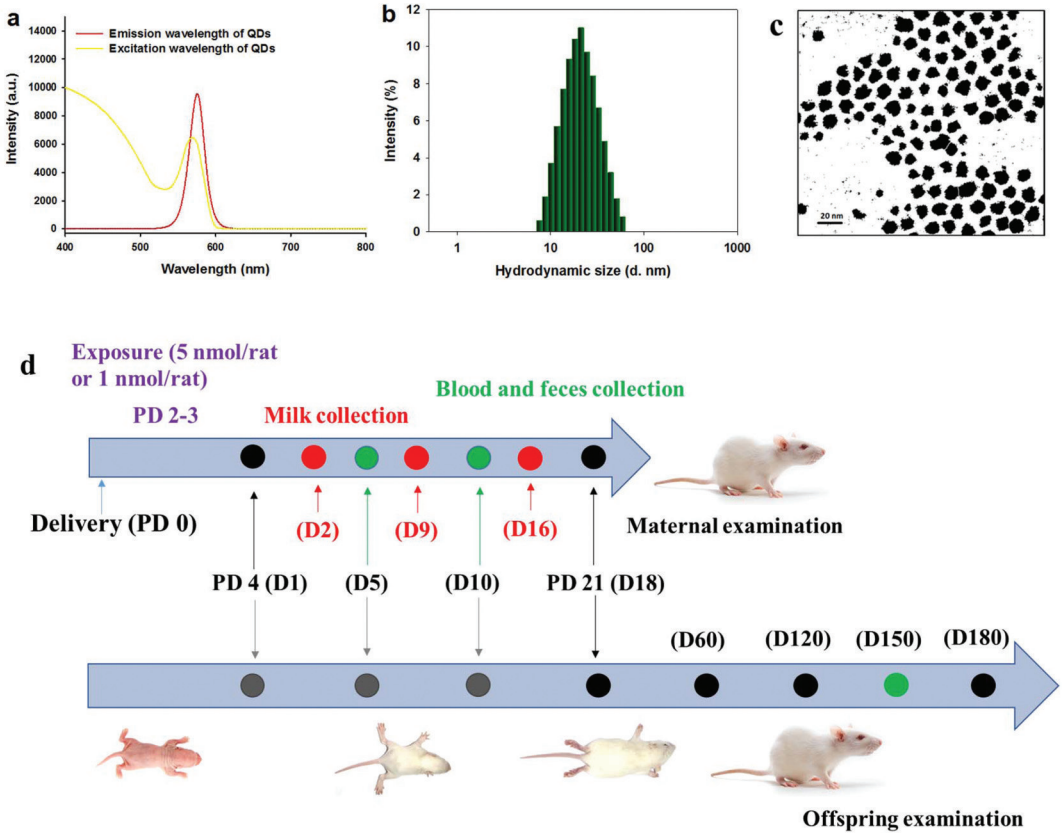

Fig. 1 Characterization of QDs (a–c) and flow diagram of the experiment (d). The absorption and emission spectra of QDs used in this study (a), the diameter of QDs determined using DLS (b) and TEM (c). The PD0 and D1 mean data were collected at postnatal day 0 and 1 day post injection (dpi), respectively.

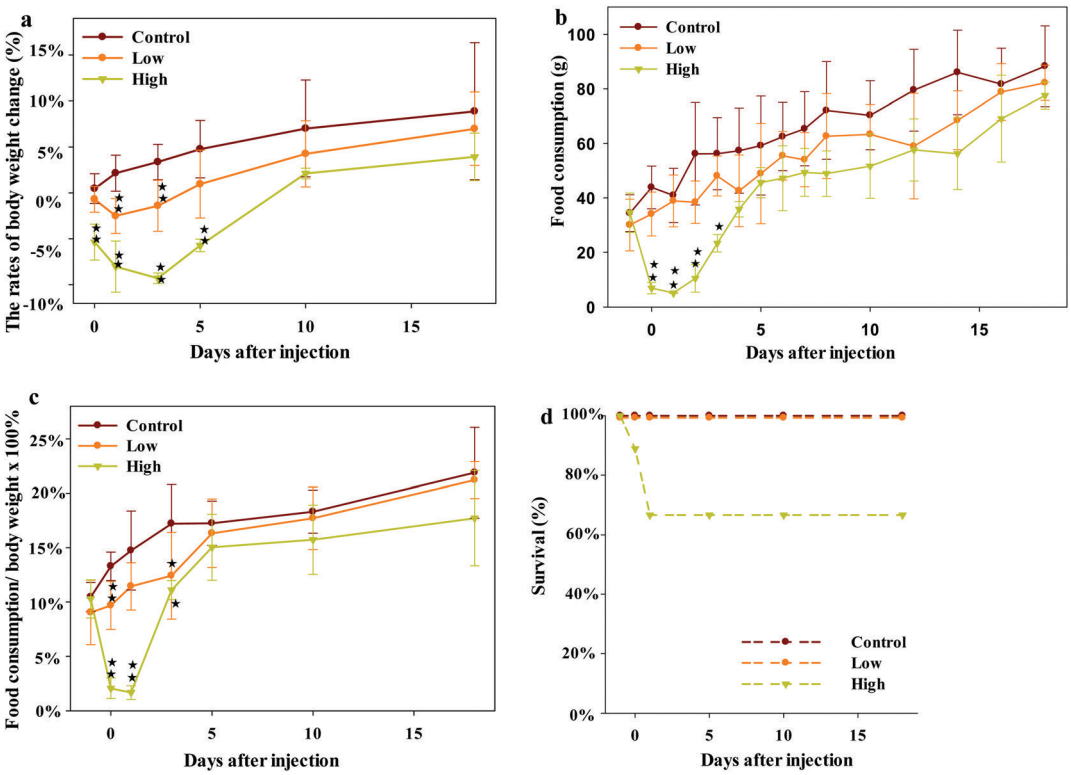

Fig. 2 Rates of body weight change (a), food consumption (b), food consumption/body weight (c), and survival rate (d) of maternal rats following intravenous injection of QDs in doses of 5 nmol (high) or 1 nmol (low) at postnatal day 2 (PD2) and PD3. n = 3.

group was impaired. In addition, the rate of food consumption compared to the temporary BW should provide more accurate data than that from merely measuring the food intake as food consumption is dependent on the BW. The rate of food intake/BW (9.67 ± 2.21%) between the first injection and the second injection in the low-dose group was extremely smaller than the rate (13.29 ± 1.31%) in the control group (Fig. 2c), which was not found in terms of the food consumption alone. A significant increase in the spleen index of dams in the high-dose group implied the occurrence of splenomegaly, while the other organs showed no significant variations in mass (Table S2†). Rats in the high-dose group also exhibited less activity and feeding behaviors.

QDs with similar sizes to large proteins or viruses can interact with the blood and blood components following i.v. administration, which may induce inflammatory, immune responses, and alter related hematological factors in the blood, such as the white blood cell count (WBC).[19,20,49] Consequently, representative hematology parameters, including WBC, red blood cells count (RBC), hemoglobin (HB), mean corpuscular hemoglobin (MCH), corpuscular hemoglobin concentration (MCHC), polymorphomultinuclear neutrophil granulocyte (PMN), lymphocyte (LY), hematocrit, and platelet count (PLT) were counted (Fig. 3 and Fig. S1†). The numbers of PMN and WBC were increased at four time points in both the QD-treated groups, whereas a statistical significance was only found in the low-dose group at 1 dpi. Variations in PMN and WBC indicated that QDs exposure caused an acute inflammatory response. MCH and MCV in the high-dose group showed significant increases at 18 dpi compared to the control group. No significant changes were observed for RBC (Fig. S1a†), while the number of was extremely PLT decreased in the high-dose group at 1 dpi, but then was elevated over time. PLT may be a sensitive marker in NPs perturbation *in vivo* according to our work[49] and several other research studies.[50,53,54] Other indicators, such as HB, hematocrit, MCHC, and LY, showed mild changes (Fig. S1†). Several sensitive markers of liver function, such as alanine aminotransferase (ALT), aspartate aminotransferase (AST), direct bilirubin (DBIL), and gamma glutamyl transaminase (GGT), were determined. As shown in Fig. 3e, f, g, and h, the levels of ALT, AST, DBIL, and GGT in the high-dose group greatly exceeded the normal ranges at 1 dpi and 5 dpi, indicating severe hepatocellular injuries resulting from a high liver accumulation of the QDs, albeit these indicators fell back to the normal range by 10 dpi and 18 dpi, implying that the liver damage was attenuated. Other liver and kidney function indicators are shown in Table S3,† where dose-dependent decreases in total protein (TP), albumin (ALB), and globulin (GLB) were observed in the first two time points, which also returned to normal later. Creatinine (CRE), blood urea nitrogen (BUN), and urea (UA) also showed different changes at various time points and in the different treatment groups, suggesting an impairment of the renal function.

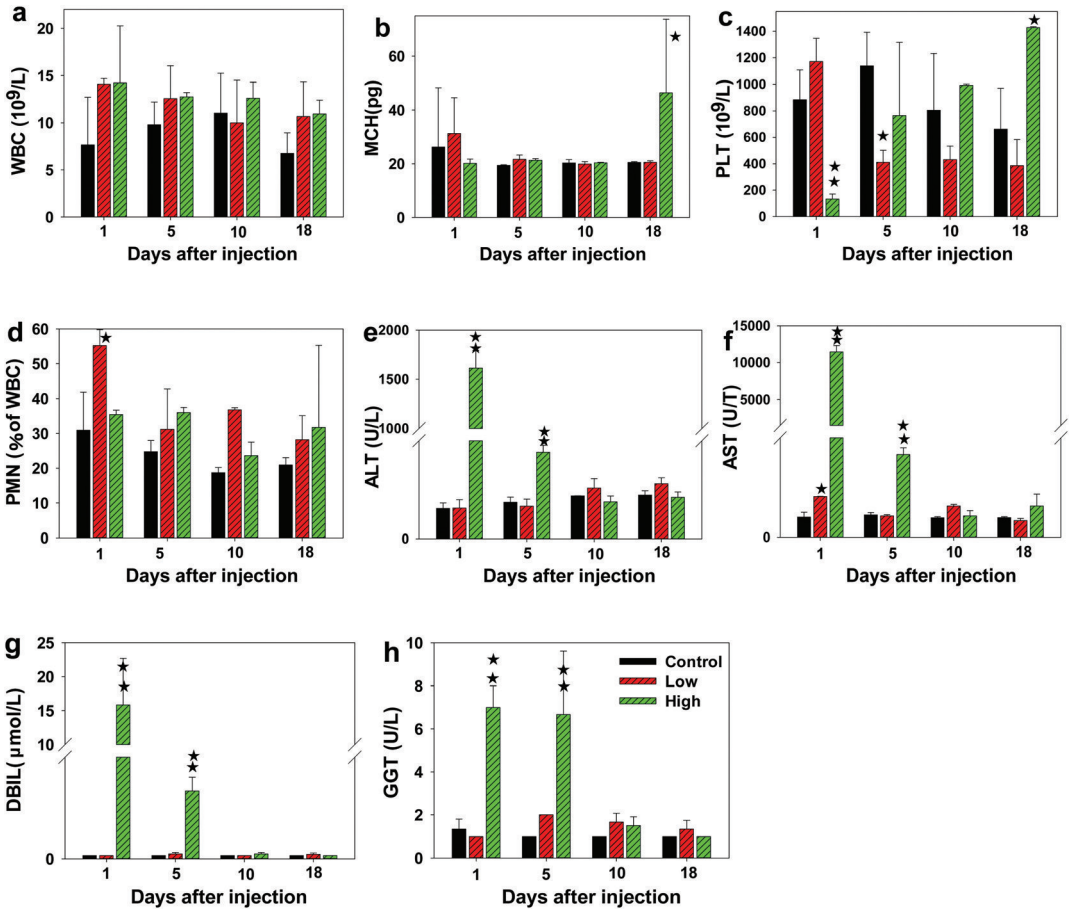

Fig. 3 Typical whole blood and serum indicators from maternal rats treated with 5 nmol (high) or 1 nmol (low) of QDs and vehicle control. (a–h) Results exhibit mean and standard deviation of white blood cells count, WBC (a); mean corpuscular hemoglobin, MCH (b), platelet count, PLT (c), polymorphomultinuclear neutrophil granulocyte PMN (d), alanine aminotransferase, ALT (e); aspartate aminotransferase, AST (f); direct bilirubin, DBIL (g), and gamma glutamyl transaminase, GGT (h). n = 3.

An histology examination was performed as it can provide more macroscopic organ and visual evidence, which is more accurate in the evaluation of acute systemic toxicity, to support the serum biochemistry findings that indicated liver and kidney damage. In the control group, the liver, spleen, and kidney had no apparent pathological abnormalities. A minimal focal inflammatory cell infiltration, nucleus vacancy or deformation, and small vesicle-like cytoplasm in partial hepatocytes in the liver, hyperemia, hyperplasia in the lymph nodule in the spleen, and inflammatory cell infiltration, renal tubular epithelial cell exfoliation in the kidney were observed in the low-dose group at 1 dpi. However, severe cellular apoptosis and necrosis, cytolysis, large cavity, blurred hepatic sinus borderline, integrity and morphology loss of hepatic lobules in the liver, white and red pulp aberrations, damaged splenic nodule, evident hyperplasia, nucleus and cytoplasm disintegration in the spleen, severe renal tubular epithelial cell necrosis, vacuolar degeneration, stretched cytoplasm and condensed nucleus, incomplete glomerulus, and tubules structures in the kidney were observed in the high-dose group (Fig. 4). These findings verified the dose-dependent changes in histopathology caused by the QDs. However, these changes diminished or disappeared by 18 dpi, which only showed minimal cellular edema and endothelial cell aggregation in the liver and mild hyperplasia and swelling of glomerular capillary endothelium in the kidney in both QDs-treated groups, with no or low pathological changes in the spleen in the low- and high-dose groups (Fig. 4). Decreases in hepatocellular damage should account for the diminished levels of ALT, AST, DBIL, and GGT in the circulation. Furthermore, lung exposure to high-dose QDs presented enlarged airway cavities, substantial loose cytoplasm, and a thinning alveolar cell layer at 1 dpi, but these changes were attenuated by day 18. Some cavities and thin alveolar walls were observed in the lungs at 1 dpi in comparison to negligible injury at 18 dpi in the low-dose group (Fig. S3†). Fig. S3† also shows that the heart, uterus, brain, and intestine were further examined and demonstrated changes, including cavities, cell edema and cytoplasm distortion, occurred only in the high-dose group at 1 dpi.

Recently, several studies have demonstrated that 0.1–30 μg per mouse of single-wall carbon nanotubes induce fetal malformations and miscarriages,[43] while 50 μg per mouse of QDs

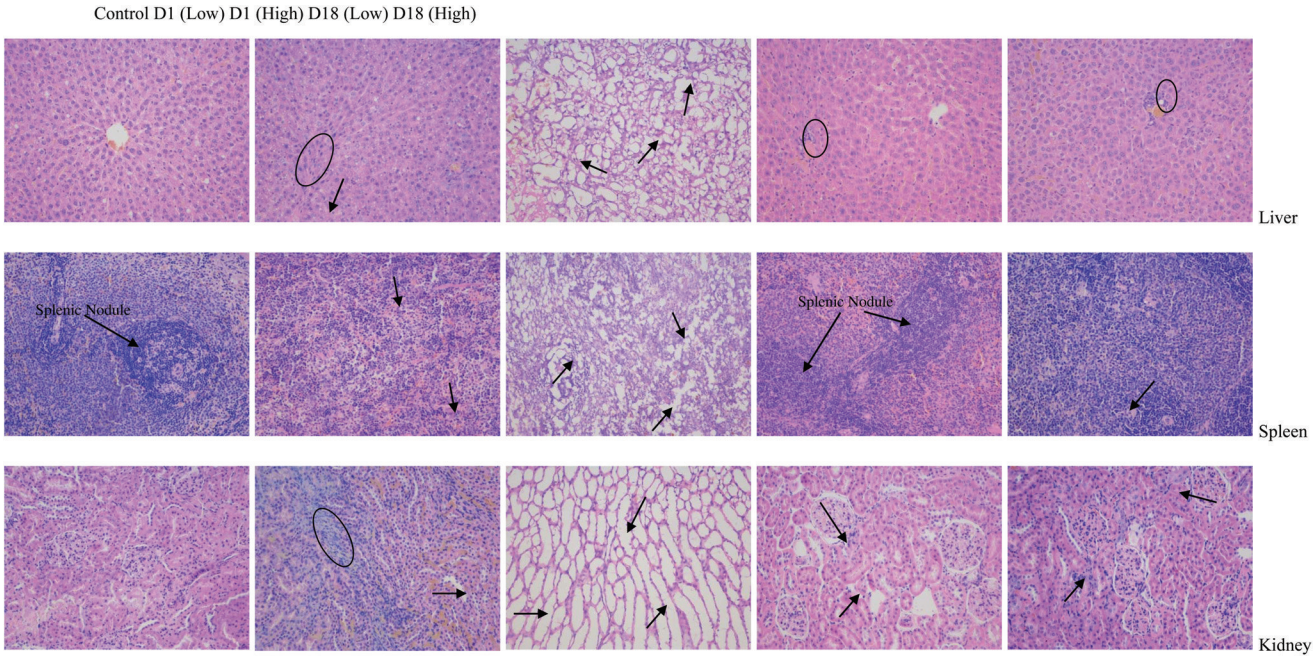

Fig. 4 Histological images of maternal rat's liver, kidney, and spleen on 1 (D1) and 18 (D18) dpi. Arrows indicate structural damages on both treated rat organs. n = 3.

triggered fetal death in the uterus,[26] and 800 μg per mouse of silica nanoparticles caused fetal resorption and restricted fetal growth.[23] However, these reports failed to measure the levels of sex hormones, which are of central importance to placenta and ovarian functions and mammogenesis during an animal's gestation and galactosis periods.[36] Meanwhile, Jain *et al.* reported that cadmium-containing NPs could be considered as endocrine disruptors triggering estrogenic responses and increasing the uterine weight.[55] The concentrations of P_4, FSH, E_2, PRL, and LH in maternal rats were therefore evaluated (Table 1). PLR could promote the development of mammary glands, and cause and sustain lactation, while P_4 could facilitate the growth of mammary gland flocculus and acini. QDs induced significant decreases in P_4 in both groups at 1 dpi. By contrast, the levels of P_4 sharply increased to 55.4 ± 26.01 nmol L^{-1} and 139.36 ± 0.97 nmol L^{-1} at 18 dpi in the low- and high-dose groups, respectively. Furthermore, a high dosage of QDs inhibited E_2 and LH levels at 1 dpi, while FSH and PRL levels were not affected at both time points. The variations in P_4, E_2, and LH levels proved that the QDs interrupted the endocrine function. All the data gathered demonstrated that an early postnatal exposure to QDs induced severe acute systemic toxicity in maternal rats. The systemic toxicity was found to be dose-dependent and could be diminished over time, and 5 nmol of QDs induced severe acute toxicity, including BW decrease, food intake shrinkage, liver, kidney and spleen injury and inflammation, and hormones disruption, to account for the rat death.

Distribution of QDs in maternal tissues

To further verify the argument responsible for the acute animal death and to understand the toxicokinetics of QDs, Cd concentrations in the multiple tissues at 1 dpi and 18 dpi were quantitatively measured using ICP-MS. Initially, the Cd levels in the blood in low-dose group and the control group at all the time points were negligible, *i.e.*, below the detection limit, while the blood Cd level in high-dose group increased over time and peaked at 0.064 ± 0.019 μg g^{-1} at 18 dpi (Table S4†). Previous studies found that Cd levels in blood and plasma decreased over time and were below the detection limit at

Table 1 Sex hormones were evaluated with serum levels of estradiol (E_2), progesterone (P_4), luteinizing hormone (LH), follicle stimulating hormone (FSH), prolactin (PRL). D1 and D18 mean the data were collected at 1 and 18 dpi, respectively

	D1			D18		
Parameters	Control	Low	High	Control	Low	High
P_4 (nmol L^{-1})	67.59 ± 6.01	32.63 ± 25.07*	20.08 ± 1.49*	17.2 ± 3.27	55.4 ± 26.01**	139.36 ± 0.97**
FSH (IU L^{-1})	4.4 ± 0.63	2.56 ± 0.34	5.39 ± 3.59	5.35 ± 2.84	3.72 ± 1.39	3.18 ± 0.87
E_2 (pmol L^{-1})	10.55 ± 0.94	7.43 ± 5.48	3.5 ± 1.75*	14.55 ± 9.64	19.73 ± 9.46	10.35 ± 0.05
PRL (μg L^{-1})	9 ± 2.81	6.78 ± 2.32	7.69 ± 3.20	8.61 ± 5.21	12.37 ± 2.48	7.98 ± 5.25
LH (IU L^{-1})	9.29 ± 1.28	6.89 ± 2.71	4.1 ± 0.44*	7.72 ± 1.47	5.97 ± 2.23	5.12 ± 1.16

3 dpi and 7 dpi following 0.2 μmol kg^{-1} and 12 μg per mouse administrations.[56,57] Herein, the incremental level of Cd in this study could be attributed to the high-dose exposure and QDs degradation, which released Cd ions that subsequently entered into the blood circulation, as proposed by relevant research studies.[20,56] The excretion of Cd from feces was only observed at 1 dpi but not at other time points in both groups, suggesting the QDs were not effectively excreted through the biliary pathway from the liver to the bile duct, intestine, and feces. This finding also concurred with literature reports.[17,52,57,58]

Fig. 5 and Table S5† show that the organ Cd level in the control group was below the detection limit except for 0.047 ± 0.009 μg g^{-1} in the kidney and 0.174 ± 0.009 μg g^{-1} in the intestine. Endogenous Cd in the control group cannot be neglected, such as approximately 10 μg g^{-1} of Cd detected in the kidney of control monkeys,[20] because of a higher detection sensitivity and occupational exposure, and food, water, and padding contamination. At 1 dpi, the highest Cd concentrations, arranged in decreasing order, were found in the liver, spleen, kidney, lung, uterus, stomach, breast, heart, and brain tissues in the low-dose group. For the high-dose group, however, Cd was primarily accumulated in the spleen and lung with values of 14.56 ± 5.98 μg g^{-1} and 11.61 ± 5.50 μg g^{-1}, which were approximately 15.6 and 21.3 times higher than the corresponding doses in the low-dose group. The liver and kidney had higher Cd concentrations, followed by the intestine, uterus, breast, heart, stomach, and brain. The Cd levels in some organs (heart and uterus) increased over time, most strikingly elevated in the kidney, in which the concentrations of Cd sharply increased from 0.71 ± 0.31 μg g^{-1} to 12.51 ± 0.44 μg g^{-1}, and 5.41 ± 3.64 μg g^{-1} to 42.31 ± 1.68 μg g^{-1}, respectively. Also, the liver and spleen showed increased Cd levels in the low-dose group in comparison with the steady levels in the high-dose group. Surprisingly, the Cd levels in the lungs and breasts of the two treatment groups displayed an opposite trend. For instance, Cd levels in the breast in the high-dose group dropped from 0.474 ± 0.042 μg g^{-1} to 0.332 ± 0.106 μg g^{-1}, while the level increased from 0.053 ± 0.018 μg g^{-1} to 0.163 ± 0.043 μg g^{-1} in the low-dose group.

Meanwhile, we also calculated the percentages of Cd in multiple tissues and found the total recovery rates of QDs injection dose were 43.66% and 54.25% at 1 dpi, and 109.06% and 63.47% at 18 dpi in the low- and high-dose groups, respectively (Table 2). The gap in QDs recovery could be attributed to variations in the injection, mouse body metabolism, *etc*. The residual Cd mass could be retained in the carcass, as previous studies also proved that 40–50% QDs were mainly distributed in the large masses of the muscle, skin, bone, and so on.[17,57] Early predominant deposition in the liver and spleen was expected due to the clearance of QDs from the blood by resident phagocytes of the MPS, as supported from literature.[49–52,58] A substantial increment of the Cd level in the kidney at 18 dpi in both exposure groups (Table 2) verified previous work using PEG-coated CdSe/ZnS QDs.[17,19] This indicates that the carboxyl-coated CdSe/ZnS QDs used here might partially undergo degradation *in vivo* and release free Cd ions, which are then absorbed by the kidney.[56,57] The QDs core and shell must, however, remain largely intact as the detectable fluorescence lasts over weeks to months and there is slight accumulated differences in their constitutions (*e.g.*, Cd, Se, Zn) in various organs.[18,19] Noticeably, the Cd lung burden (5.67%) at 1 dpi in the 5 nmol per rat QDs exposure group was extremely much higher than the value of 1.13% in the 1 nmol per rat QDs group and 0.6% and 0.01 ± 0.03% in recent studies,[17,57] implying that QDs might quickly accumulate and form aggregates with proteins or cells and then induce a severe pulmonary embolism, subsequently leading to acute animal death following exposure.[50] Furthermore, the accumulations of Cd/QDs in the uterus and breast pose high risks to the embryo or infant growth and development. Taken together, these findings demonstrate that the QDs were not effectively eliminated from the body and a large amount of QDs/Cd accumulation occurred *in vivo*, suggesting the QDs could transmit to breast milk *via* the blood circulation and translocate to the offspring *via* breastfeeding during the lactation period.[59]

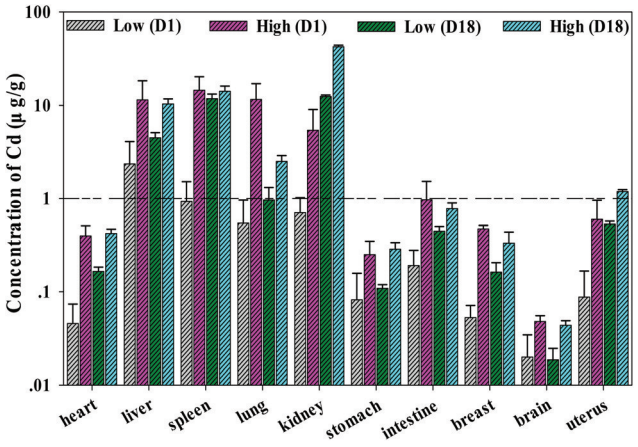

Fig. 5 Biodistribution of QDs/cadmium in maternal rats after postnatal exposure (at PD2 and PD3) to QDs. D1 and D18 mean data were collected at 1 and 18 dpi, respectively. n = 3.

Table 2 The percentage of Cd content in major tissues of two dosage QDs injected rats at 1 (D1) and 18 (D8) dpi

	Proportion of injected dose (%)			
Tissues	Low (D1)	High (D1)	Low (D18)	High (D18)
Liver	40.00	40.27	64.48	39.43
Kidney	1.45	2.85	32.53	17.37
Spleen	0.79	5.01	9.71	4.96
Lung	1.13	5.67	1.96	1.05
Heart	0.09	0.11	0.30	0.13
Brain	0.04	0.02	0.03	0.02
Uterus	0.16	0.24	0.05	0.19
Blood	0	0.08	0	0.30
Total recovery	43.66	54.25	109.06	63.47

Milk transmission of QDs and their distribution in offspring

To the best of our knowledge, this is the first attempt to determine whether QDs enter the breast milk and transfer to the offspring *via* breastfeeding or not. In recent studies, Huang *et al.*[39] found multi-walled carbon nanotubes crossed the blood-placenta barrier and induced brain deformity or slowed the BW depending on the p53 genotype. Bai *et al.*[60] demonstrated that nanotubes were stored in the testes 24 h after injection, and induced reversible oxidative stress and tissue damage. Silica NPs transferred to the placenta, fetal liver, and fetal brain and caused smaller uteri and fetuses, as proved by Yamashita *et al.*[23] In spite of the evaluation of NPs reproductive toxicity on pregnant mice and male mice, those studies ignored the puerperium animals as well as the total contents of NPs in the fetus. The breast milk samples at 2, 9, and 16 dpi, the stomach with milk, and the intestine, liver, spleen, and kidney of infants at 1, 5, 10, and 18 dpi were thus obtained in this study. No milk was harvested from the high-dose group because three rats unexpectedly died. Fig. 6a and Table S6† show that at 2 and 16 dpi, the Cd concentrations in the milk from the low-dose group were 29.55 ± 17.72 ng g^{-1} and 39.28 ± 17.72 ng g^{-1}, respectively, which were significantly higher than the concentrations (5.64 ± 0.55 ng g^{-1} and 19.55 ± 5.55 ng g^{-1}) in the control group. Contrastingly, no significant change in the Cd level was found in the milk at 9 dpi compared with the control group. The intestine Cd contents in both exposure groups did not differ from that in the control group at 1 dpi, but a dose-dependent accumulation of Cd in the offspring's intestine was found after 5 dpi (Fig. 6b). For instance, the Cd concentrations were 168.23 ± 56.23 ng g^{-1} and 198.27 ± 43.76 ng g^{-1} at 10 dpi, and significantly higher than 103.24 ± 33.25 ng g^{-1} in the control group. Furthermore, the stomach Cd levels were significantly increased in high-dose group at 5 and 10 dpi over the control group (Fig. 6c). The liver, spleen, and kidney Cd contents in both exposure groups, however, showed no significant differences compared with those of the control group at 1, 5, 10, and 18 dpi (Fig. 6d and Table S7†). It was hypothesized that a very small amount of QDs/Cd therefore enters the offspring and is absorbed by the intestine, but these particles or ions cannot be uptaken by the MPS, mainly due to the underdeveloped intestine, and thus they are excreted directly. However, no available data exists to support this view, which requires further investigation. Additionally, the Cd concentrations in the offspring's intestine, liver, spleen, and kidney were measured up to 180 dpi, and no significant differences were found among these groups at 60, 120, and 180 dpi. The absolute Cd tissue concentrations are given in Table S7.† On the other hand, 3-mercaptopropionic acid-coated QDs containing 50 μg of Cd had 13.20 ± 3.24 ng g^{-1} Cd/QDs entrance to the embryo, which caused fetal death.[26] The possible side effects on offspring growth and development were thus evaluated.

Long-term effects on offspring growth and development

Exposure to QDs caused acute systemic toxicity in dams, and a small amount of QDs was transferred to the offspring *via* breastfeeding. Acute and long-term toxicity in the offspring was examined up to 180 days after exposure. The growth restriction of the offspring was observed in both exposure groups. After the first injection (0 dpi), the infant BW in the

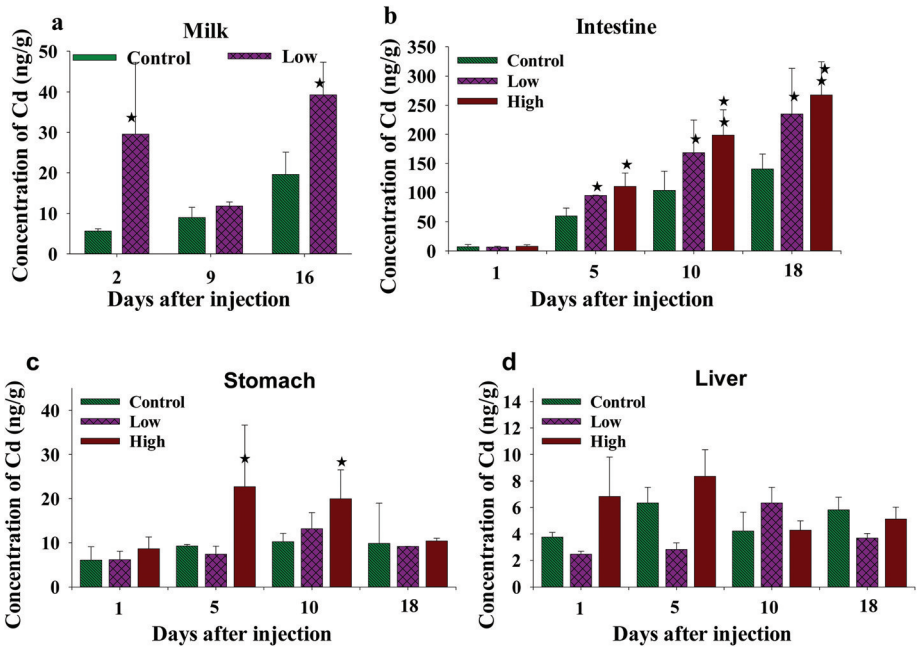

Fig. 6 Cadmium concentrations in maternal breast milk (a) and offspring intestine (b), stomach (c), and liver (d) at 1–18 dpi. D1 and D18 mean data were collected at 1 and 18 dpi, respectively. n = 3.

high-dose group decreased slightly and were significantly lower than those in the control group. Afterward, the infant BW in the high-dose group showed the slowest increase throughout the lactation period compared with those in the low-dose and control groups. The infant BW in the low-dose group started to show a negative effect on BW increase at 3 dpi, persisting till 15 dpi (Fig. 7a). Also, at 60 dpi, when the offspring was mature, the BW in both treated groups were inferior to those in the control group, and the differences were statistically significant (Table S8†). However, the variations in BW after 90 dpi were not evident. The infants' death occurred within 3 dpi only in the high-dose group, with approximately a 28.92% survival rate (Fig. 7b). The offspring body form and morphology in the low-dose group were smaller than those in the control group, as shown in Fig. 7c. No malformation was observed in offspring throughout the period. At least four descendant rats, including female and male rats, were sacrificed, and various organs were removed for evaluation of the visceral index at 60, 120, and 180 dpi. The liver, kidney, heart, brain, and testis showed no significant differences in mass in comparison with those in the control group at all time points. The lung weighed significantly less in both administration groups, while the uterus exhibited a significant weight increase in the high-dose group at 120 dpi (Table S8†).

Hematology parameters, including WBC, MCH, PLT, PMN, RBC, HB, hematocrit, MCV, MCHC, and LY, were determined at 18, 150, and 180 dpi and the results are listed in Fig. 8 and Fig. S2.† These hematological markers, including MCH RBC, HB, hematocrit, MCV, MCHC, and LY, in both QDs treatment groups remained at similar levels compared with the control group. Minimal changes in WBC, PMN, and PLT, which were not statistically different from the control group, were observed. Several crucial biochemical indicators, consisting of ALT, AST, DBIL, GGT, and BUN, were measured at 18, 60, 120, 150, and 180 dpi (Table S9†). As shown in Fig. 8, the offspring showed significantly increased levels of ALT at 120 dpi in the high-dose group and DBIL at 18 dpi in both administration groups. The levels of GGT exhibited variations at 18 dpi and 120 dpi in the high-dose group. But these changes remained

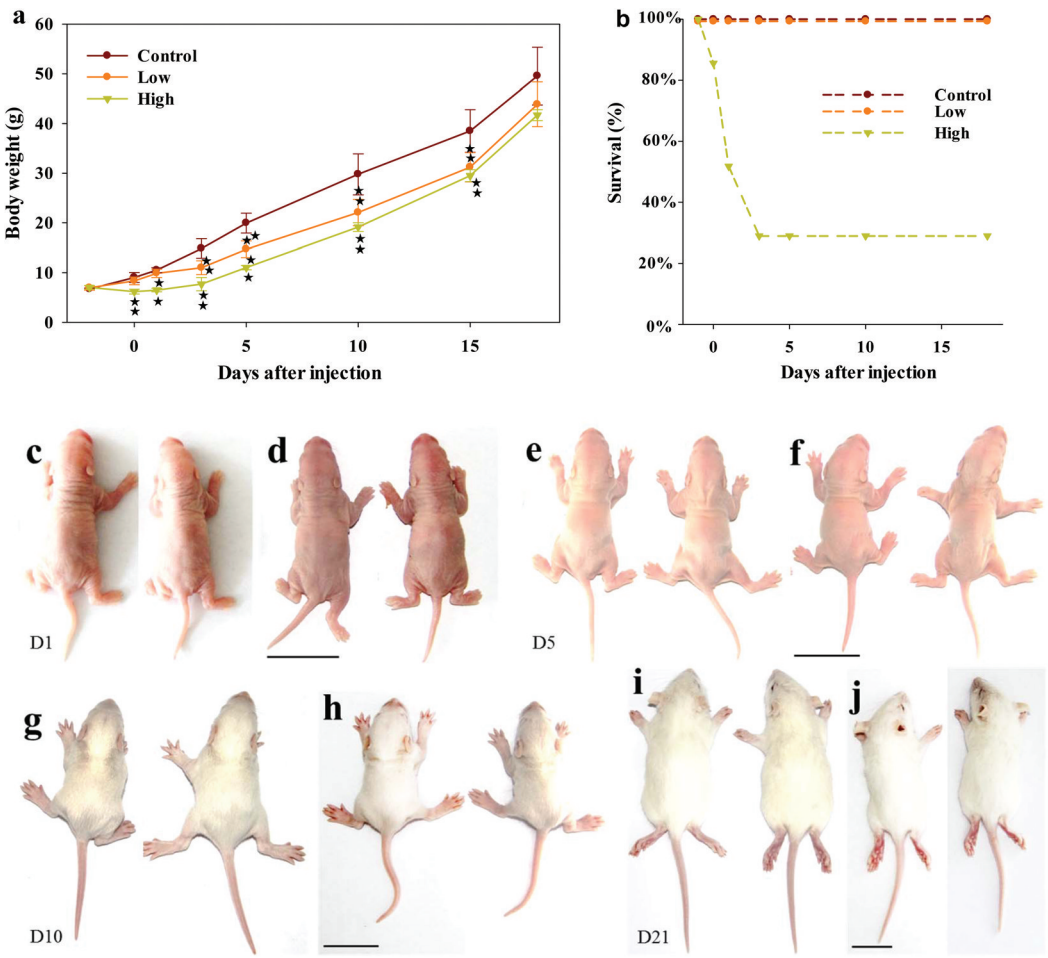

Fig. 7 Body weights (a), survival rates (b), and the growth images (c–j) of offspring are shown from day 1 to day 21 after maternal exposure to 5 nmol (high) or 1 nmol (low) of QDs and vehicle control. (c), (e), (g), and (i) exhibit the offspring in the vehicle control and (d), (f), (h), and (j) show the offspring in the low-dose group (1 nmol) at 1, 5, 10, and 21 dpi (D1, D5, D10, and D21). The offspring in the high-dose group are not shown due to partial offspring death. The scale bar is 2.5 cm. n = 4.

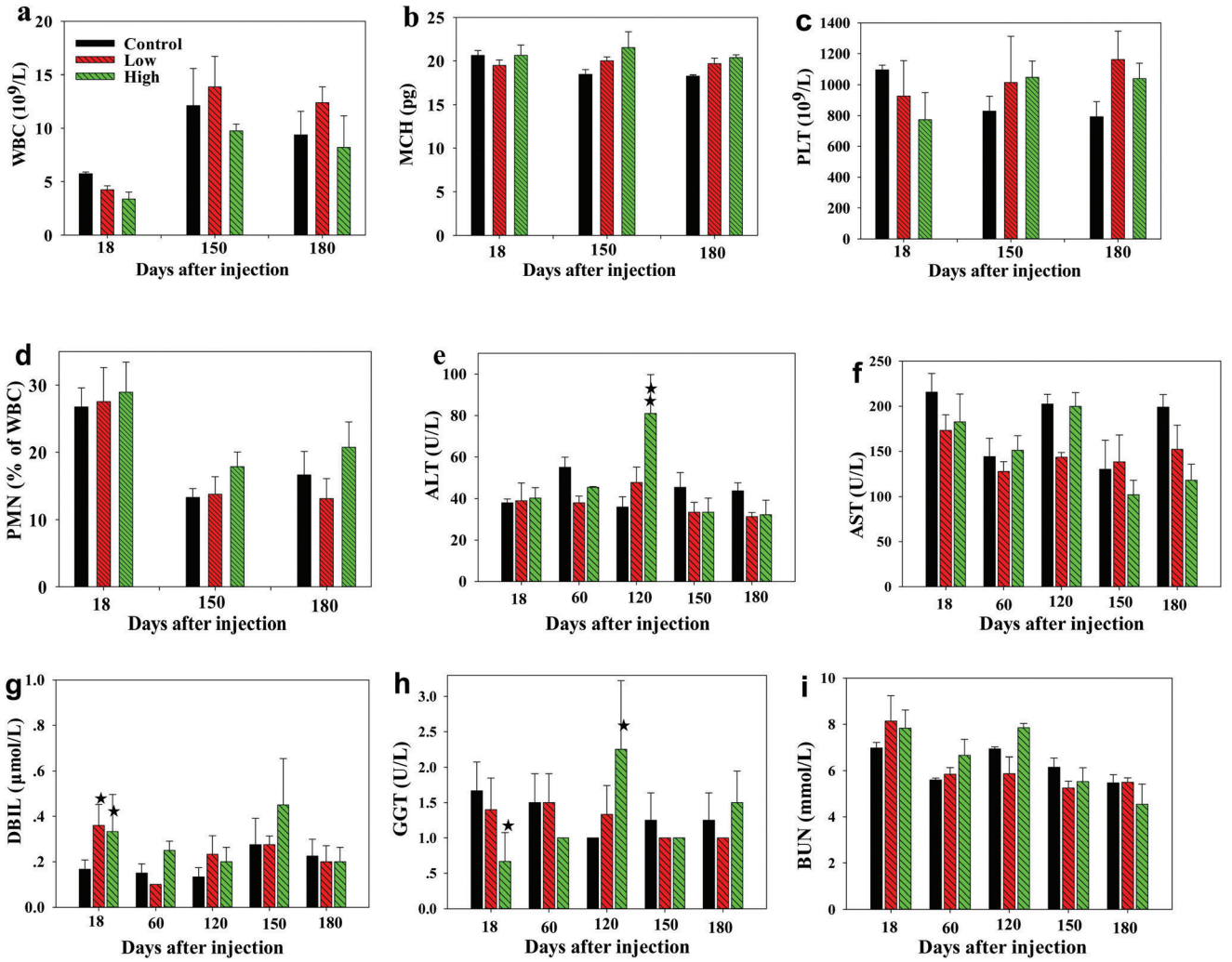

Fig. 8 Typical whole blood and serum indicators of the offspring in 5 nmol of QDs group (high) or 1 nmol of QDs group (low) and the vehicle control at 18, 60, 120, 150, and 180 dpi. (a–i) Results exhibit mean and standard deviation of white blood cells count, WBC (a); mean corpuscular hemoglobin, MCH (b), platelet count, PLT (c), polymorphomultinuclear neutrophil granulocyte PMN (d), alanine aminotransferase, ALT (e); aspartate aminotransferase, AST (f); direct bilirubin, DBIL (g), gamma glutamyl transaminase, GGT (h) and blood urea nitrogen, BUN (i). n = 3.

in the normal ranges based on the literature records.[19,20,49,51] Further investigation of the potential toxicity on offspring from maternal exposure to QDs through histopathological examination of the organs was performed. The possible Cd absorbed, stored, and eliminated by the organs, including the intestine, liver, spleen, and kidney, were collected, fixed, stained, and analyzed at 18, 60, 120, 180 dpi. Luckily, no apparent tissue or cell damage was observed in the liver, spleen, and kidney throughout the entire experiment. Normal hepatocytes in the liver, no hyperplasia in the spleen, and an intact glomerulus structure in kidney were observed. However, the intestines in the high-dose group exhibited epithelial cell edema and loose cytoplasm at 120 dpi. More organs were evaluated (Fig. S4†) and no pathological lesions or abnormalities were found.

In prenatal exposure to NPs, the embryo or fetus could be influenced *via* three approaches: (1) NPs or impurities that translocate through the placenta, (2) impaired placental structure and function, and (3) circulating cytokines or other secondary messengers from an inflammatory process in dams. Also, we speculated that both the low quality and quantity of breast milk and NPs transmitted to the neonates were responsible for the offspring developmental retardation. A limitation of this study is that only the negatively charged carboxyl-coated CdSe/ZnS QDs were applied to the lactating mice. Future studies could thus concentrate on determining the effects of the QDs characteristics, such as surface chemistry, NPs size, and NPs composition. On their translocation ability and toxicity profiles.[30,45,50] Neutral charged QDs, like PEG-QDs, have a relative longer plasma half-time,[34,49] while bovine serum albumin (a common protein in serum)-coated QDs was cleared faster from blood than mercaptoundecanoic acid-coated QDs.[58] Silica shell was considered to reduce QDs transfer from pregnant mice

to embryos.[26] Moreover, the translocation mechanism of QDs crossing the blood–milk barrier, genotoxicity, and proteomics evaluation, especially subtle changes *in vivo*, such as oxidative stress, are required for further exploration to comprehensively understand the QDs nanotoxicology (Fig. 9).

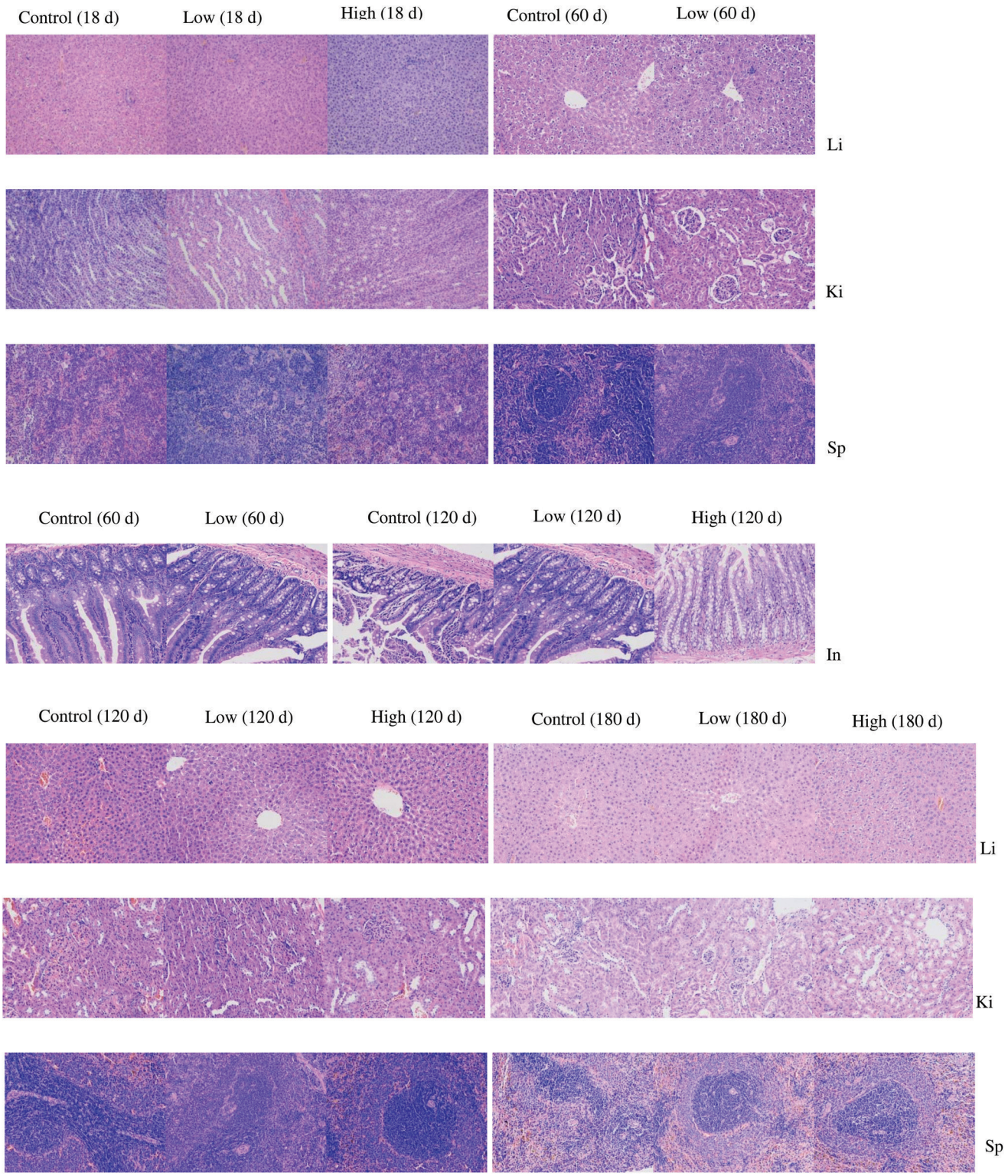

Fig. 9 Histological images of the offspring's liver, kidney, spleen, and intestine at 18, 60, 120, and 180 dpi. Arrows indicate structural damages on both treated rat's organs. $n = 3$.

Conclusion

This study demonstrated that the dose-dependent acute systemic toxicity of QDs exposure in lactating rats with a high dose (5 nmol per rat) of QDs causes severe toxicities, including splenomegaly, multiple organ injuries and inflammation, and endocrine disruption, and rat death, while slight toxic effects with mild weight decreases, mild hematology, serum biochemistry, and histopathological changes were observed in the low-dose group (1 nmol per rat). The dose-dependent accumulation and QDs redistribution and resorption in various organs were evident, suggesting the QDs experienced translocation or degradation *in vivo*. This phenomenon was further proved by the higher contents of cadmium found in the breast milk and stomachs and intestines of the offspring in the treated groups. Notably, a very small amount of QDs/Cd was translocated to the intestines of offspring during breastfeeding, but these particles or ions cannot be absorbed by the MPS (*e.g.*, liver, spleen) and kidney from birth up to 180 dpi. Furthermore, a high dose of QDs lead to severe growth inhibition, and offspring death, but long-term growth restriction (within 90 days) was also found in the low-dose group. Additionally, the hematology, serum biochemistry, and histology results showed minimal side effects against survival offspring in the long term. This investigation provides evidence that lactating animals are more susceptible to QDs exposure and potential fetotoxicity studies of these and other NPs with improved methods therefore are stilled needed.

Conflicts of interest

The authors declare no competing financial interests.

Acknowledgements

This work was supported by National Natural Science Foundation of China (81560537). The authors would like to thank Dr Andrew Wang and Dr Hong Xu for providing valuable information and the materials of the QDs.

References

1 A. M. Smith, H. Duan, A. M. Mohs and S. Nie, *Adv. Drug Delivery Rev.*, 2008, **60**, 1226–1240.
2 T. Jamieson, R. Bakhshi, D. Petrova, R. Pocock, M. Imani and A. M. Seifalian, *Biomaterials*, 2007, **28**, 4717–4732.
3 X. Gao, Y. Cui, R. M. Levenson, L. W. Chung and S. Nie, *Nat. Biotechnol.*, 2004, **22**, 969–976.
4 P. Juzenas, W. Chen, Y.-P. Sun, M. A. N. Coelho, R. Generalov, N. Generalova and I. L. Christensen, *Adv. Drug Delivery Rev.*, 2008, **60**, 1600–1614.
5 D. R. Larson, W. R. Zipfel, R. M. Williams, S. W. Clark, M. P. Bruchez, F. W. Wise and W. W. Webb, *Science*, 2003, **300**, 1434–1436.
6 I. L. Medintz, H. T. Uyeda, E. R. Goldman and H. Mattoussi, *Nat. Mater.*, 2005, **4**, 435–446.
7 X. Michalet, F. F. Pinaud, L. A. Bentolila, J. M. Tsay, S. Doose, J. J. Li, G. Sundaresan, A. M. Wu, S. S. Gambhir and S. Weiss, *Science*, 2005, **307**, 538–544.
8 P. Zrazhevskiy and X. Gao, *Nat. Commun.*, 2013, **4**, 1619.
9 T. M. Samir, M. M. Mansour, S. C. Kazmierczak and H. M. Azzazy, *Nanomedicine*, 2012, **7**, 1755–1769. Q4
10 M. van der Zande, R. J. Vandebriel, E. Van Doren, E. Kramer, Z. Herrera Rivera, C. S. Serrano-Rojero, E. R. Gremmer, J. Mast, R. J. Peters and P. C. Hollman, *ACS Nano*, 2012, **6**, 7427–7442.
11 J. Thompson and J. Bannigan, *Reprod. Toxicol.*, 2008, **25**, 304–315.
12 Y. Qu, W. Li, Y. Zhou, X. Liu, L. Zhang, L. Wang, Y.-f. Li, A. Iida, Z. Tang and Y. Zhao, *Nano Lett.*, 2011, **11**, 3174–3183.
13 A. M. Derfus, W. C. W. Chan and S. N. Bhatia, *Nano Lett.*, 2004, **4**, 11–18.
14 B. I. Ipe, M. Lehnig and C. M. Niemeyer, *Small*, 2005, **1**, 706–709.
15 J. Lovric, S. J. Cho, F. M. Winnik and D. Maysinger, *Chem. Biol.*, 2005, **12**, 1227–1234.
16 A. Nagy, A. Steinbrück, J. Gao, N. Doggett, J. A. Hollingsworth and R. Iyer, *ACS Nano*, 2012, **6**, 4748–4762.
17 R. S. Yang, L. W. Chang, J. P. Wu, M. H. Tsai, H. J. Wang, Y. C. Kuo, T. K. Yeh, C. S. Yang and P. Lin, *Environ. Health Perspect.*, 2007, **115**, 1339–1343.
18 J. A. J. Fitzpatrick, S. K. Andreko, L. A. Ernst, A. S. Waggoner, B. Ballou and M. P. Bruchez, *Nano Lett.*, 2009, **9**, 2736–2741.
19 T. S. Hauck, R. E. Anderson, H. C. Fischer, S. Newbigging and W. C. Chan, *Small*, 2010, **6**, 138–144.
20 L. Ye, K.-T. Yong, L. Liu, I. Roy, R. Hu, J. Zhu, H. Cai, W.-C. Law, J. Liu, K. Wang, J. Liu, Y. Liu, Y. Hu, X. Zhang, M. T. Swihart and P. N. Prasad, *Nat. Nanotechnol.*, 2012, **7**, 453–458.
21 H. S. Choi, B. I. Ipe, P. Misra, J. H. Lee, M. G. Bawendi and J. V. Frangioni, *Nano Lett.*, 2009, **9**, 2354–2359.
22 H. S. Choi, W. Liu, P. Misra, E. Tanaka, J. P. Zimmer, B. Itty Ipe, M. G. Bawendi and J. V. Frangioni, *Nat. Biotechnol.*, 2007, **25**, 1165–1170.
23 K. Yamashita, Y. Yoshioka, K. Higashisaka, K. Mimura, Y. Morishita, M. Nozaki, T. Yoshida, T. Ogura, H. Nabeshi, K. Nagano, Y. Abe, H. Kamada, Y. Monobe, T. Imazawa, H. Aoshima, K. Shishido, Y. Kawai, T. Mayumi, S.-I. Tsunoda, N. Itoh, T. Yoshikawa, I. Yanagihara, S. Saito and Y. Tsutsumi, *Nat. Nanotechnol.*, 2011, **6**, 321–328.
24 S. C. Sumner, T. R. Fennell, R. W. Snyder, G. F. Taylor and A. H. Lewin, *J. Appl. Toxicol.*, 2010, **30**, 354–360.
25 M. Ema, N. Kobayashi, M. Naya, S. Hanai and J. Nakanishi, *Reprod. Toxicol.*, 2010, **30**, 343–352.
26 M. Chu, Q. Wu, H. Yang, R. Yuan, S. Hou, Y. Yang, Y. Zou, S. Xu, K. Xu, A. Ji and L. Sheng, *Small*, 2010, **6**, 670–678.

27 M. Umezawa and K. Takeda, *IOP Conf. Ser.: Mater. Sci. Eng.*, 2011, **18**(23), 232001.
28 M. Semmler-Behnke, J. Lipka, A. Wenk, S. Hirn, M. Schäffler, F. Tian, G. Schmid, G. Oberdörster and W. G. Kreyling, *Part. Fibre Toxicol.*, 2014, **11**, 33.
29 L. Campagnolo, M. Massimiani, G. Palmieri, R. Bernardini, C. Sacchetti, A. Bergamaschi, L. Vecchione, A. Magrini, M. Bottini and A. Pietroiusti, *Part. Fibre Toxicol.*, 2013, **10**, 21.
30 J. Sun, Q. Zhang, Z. Wang and B. Yan, *Int. J. Mol. Sci.*, 2013, **14**, 9319–9337.
31 P. Wick, A. Malek, P. Manser, D. Meili, X. Maeder-Althaus, L. Diener, P.-A. Diener, A. Zisch, H. F. Krug and U. von Mandach, *Environ. Health Perspect.*, 2010, **118**, 432.
32 C. A. Austin, T. H. Umbreit, K. M. Brown, D. S. Barber, B. J. Dair, S. Francke-Carroll, A. Feswick, M. A. Saint-Louis, H. Hikawa and K. N. Siebein, *Nanotoxicology*, 2012, **6**, 912–922.
33 A. M. Z. Boisen, C. L. Nellemann, U. B. Vogel and H. Wallin, National Research Centre for the Working Environment.
34 H. Yang, C. Sun, Z. Fan, X. Tian, L. Yan, L. Du, Y. Liu, C. Chen, X.-j. Liang and G. J. Anderson, *Sci. Rep.*, 2012, **2**.
35 M. Shimizu, H. Tainaka, T. Oba, K. Mizuo, M. Umezawa and K. Takeda, *Part. Fibre Toxicol.*, 2009, **6**, 20.
36 G. Gao, Y. Ze, B. Li, X. Zhao, T. Zhang, L. Sheng, R. Hu, S. Gui, X. Sang and Q. Sun, *J. Hazard. Mater.*, 2012, **243**, 19–27.
37 P. Jackson, K. S. Hougaard, A. M. Z. Boisen, N. R. Jacobsen, K. A. Jensen, P. Møller, G. Brunborg, K. B. Gutzkow, O. Andersen and S. Loft, *Nanotoxicology*, 2012, **6**, 486–500.
38 A. M. Z. Boisen, T. Shipley, P. Jackson, H. Wallin, C. Nellemann, U. Vogel, C. L. Yauk and K. S. Hougaard, *Reprod. Toxicol.*, 2013, **41**, 45–48.
39 X. Huang, F. Zhang, X. Sun, K.-Y. Choi, G. Niu, G. Zhang, J. Guo, S. Lee and X. Chen, *Biomaterials*, 2014, **35**, 856–865.
40 Y. Cui, X. Chen, Z. Zhou, Y. Lei, M. Ma, R. Cao, T. Sun, J. Xu, M. Huo and C. Wen, *Chemosphere*, 2014, **96**, 99–104.
41 X. Tian, M. Zhu, L. Du, J. Wang, Z. Fan, J. Liu, Y. Zhao and G. Nie, *Small*, 2013, **9**, 2432–2439.
42 R. Balansky, M. Longobardi, G. Ganchev, M. Iltcheva, N. Nedyalkov, P. Atanasov, R. Toshkova, S. De Flora and A. Izzotti, *Mutat. Res., Fundam. Mol. Mech. Mutagen.*, 2013, **751**, 42–48.
43 A. Pietroiusti, M. Massimiani, I. Fenoglio, M. Colonna, F. Valentini, G. Palleschi, A. Camaioni, A. Magrini, G. Siracusa and A. Bergamaschi, *ACS Nano*, 2011, **5**, 4624–4633.
44 Y. Morishita, Y. Yoshioka, Y. Takimura, Y. Shimizu, Y. Namba, N. Nojiri, T. Ishizaka, K. Takao, F. Yamashita, K. Takuma, Y. Ago, K. Nagano, Y. Mukai, H. Kamada, S. I. Tsunoda, S. Saito, T. Matsuda, M. Hashida, T. Miyakawa, K. Higashisaka and Y. Tsutsumi, *ACS Nano*, 2016, DOI: 10.1021/acsnano.6b01782.
45 C. K. Zhang, S. M. Zhai, L. Wu, Y. H. Bai, J. B. Jia, Y. Zhang, B. Zhang and B. Yan, *PLoS One*, 2015, **10**.
46 W. Zhang, L. Yang, H. Kuang, P. Yang, Z. P. Aguilar, A. Wang, F. Fu and H. Xu, *J. Hazard. Mater.*, 2016, **318**, 61–69.
47 A. Mohammadipour, M. Hosseini, A. Fazel, H. Haghir, H. Rafatpanah, M. Pourganji and A. E. Bideskan, *Toxicol. Ind. Health*, 2013, DOI: 10.1177/0748233713498440.
48 L. Yang, H. Kuang, W. Zhang, Z. P. Aguilar, H. Wei and H. Xu, *Sci. Rep.*, 2017, **7**, 3303.
49 L. Yang, H. Kuang, W. Zhang, Z. P. Aguilar, Y. Xiong, W. Lai, H. Xu and H. Wei, *Nanoscale*, 2015, **7**, 625–636.
50 Y. Tang, S. Han, H. Liu, X. Chen, L. Huang, X. Li and J. Zhang, *Biomaterials*, 2013, **34**, 8741–8755.
51 Y. Su, F. Peng, Z. Jiang, Y. Zhong, Y. Lu, X. Jiang, Q. Huang, C. Fan, S.-T. Lee and Y. He, *Biomaterials*, 2011, **32**, 5855–5862.
52 Y. Lu, Y. Su, Y. Zhou, J. Wang, F. Peng, Y. Zhong, Q. Huang, C. Fan and Y. He, *Biomaterials*, 2013, **34**, 4302–4308.
53 Y. Zhang, Y. Zhang, G. Hong, W. He, K. Zhou, K. Yang, F. Li, G. Chen, Z. Liu and H. Dai, *Biomaterials*, 2013, **34**, 3639–3646.
54 Y. Yang, J. Lan, Z. Xu, T. Chen, T. Zhao, T. Cheng, J. Shen, S. Lv and H. Zhang, *Nanotoxicology*, 2014, **8**, 107–116.
55 M. P. Jain, F. Vaisheva and D. Maysinger, *Nanomedicine*, 2012, **7**, 23–37.
56 N. Liu, Y. Mu, Y. Chen, H. Sun, S. Han, M. Wang, H. Wang, Y. Li, Q. Xu and P. Huang, *Part. Fibre Toxicol.*, 2013, **10**, 37.
57 T.-K. Yeh, J.-P. Wu, L. W. Chang, M.-H. Tsai, W.-H. Chang, H.-T. Tsai, C. S. Yang and P. Lin, *Nanotoxicology*, 2011, **5**, 91–97.
58 H. C. Fischer, L. Liu, K. S. Pang and W. C. Chan, *Adv. Funct. Mater.*, 2006, **16**, 1299–1305.
59 Y. Zhang, Y. Bai, J. Jia, N. Gao, Y. Li, R. Zhang, G. Jiang and B. Yan, *Chem. Soc. Rev.*, 2014, **43**, 3762–3809.
60 Y. Bai, Y. Zhang, J. Zhang, Q. Mu, W. Zhang, E. R. Butch, S. E. Snyder and B. Yan, *Nat. Nanotechnol.*, 2010, **5**, 683–689.